

Dipole–Dipole Coupling between Excited Aromatic Probe Molecules and Defect Sites in Silica Gel

A. R. Leheny, N. J. Turro,

Department of Chemistry, Columbia University, New York, New York 10027

and J. M. Drake*

Exxon Research and Engineering Company, Annandale, New Jersey 08801 (Received: March 9, 1992;
In Final Form: May 11, 1992)

The direct energy transfer interaction between excited singlet aromatic molecules and peroxide lattice defect sites in silica gel is demonstrated. The nonexponential fluorescence relaxation of excited naphthalene and 2-methoxynaphthalene adsorbed to the pore surface of silica gel 60 is shown to be described by a mechanism involving dipole–dipole coupling between the molecular excited singlet states and the intrinsic defect sites of silica. The spectral overlap between the defect absorption and the adsorbate excited singlet state emission is measured. Values for the critical energy-transfer radius, R_0 , are determined to be approximately 10 Å for the probe molecules studied. The density of defects in the silica gel 60 is calculated to be 10^{20} cm^{-3} .

Introduction

The behavior of molecules adsorbed to porous substrates has interested investigators for many years.^{1–13} Aromatic molecules have been adsorbed to various silica supports, including silica gel, to determine the effects of interactions with surface groups on the photophysical properties of the adsorbates. The fluorescence relaxation of aromatic probes adsorbed to such surfaces have been found in many cases to be nonexponential.^{6–10} Several investigators have suggested that this behavior arises from site heterogeneity of the silica surface which may affect the excited-state lifetime of the adsorbed molecule. These authors have attempted to describe the relaxation dynamics using models which account for a distribution of lifetimes arising from a distribution of inequivalent adsorption sites.^{14–17} These models are not, however, supported by hole-burning measurements determining the inhomogeneous line broadening of the fluorescence.^{18,19}

In this paper, we show that the nonexponential relaxation of naphthalene and 2-methoxynaphthalene adsorbed to silica gel arises from energy transfer from the excited adsorbate molecules to defect sites in the silica gel. We have previously shown that such interactions exist for these molecules adsorbed to a silica zeolite, silicalite.²⁰ We demonstrate that the nonexponential decay of the adsorbate molecules may be described by a mechanism in which the excitation energy is transferred via a dipole–dipole mechanism to randomly distributed defect acceptors. We further show that the criterion for dipole–dipole coupling, spectral overlap between the defect absorption and adsorbate emission, is met.

The model for dipole–dipole energy transfer has been described in detail previously.^{21–23} Briefly, the reaction is



where D is the donor species, A is the acceptor, and $W(r)$ describes the hierarchical one-step energy-transfer rate that depends on the distance, r , between D* and A. The general form of the survival probability of D* may be written^{21–23} as

$$\Phi_D(t, r_0) = \exp\left(-p \int_{r_0}^{\infty} dr \rho_0(r) (1 - \exp[-W(r-r_0)t])\right) \quad (2)$$

where the position of the donor, r_0 , is excluded and p is the fraction of the total acceptor sites that is occupied. $\rho_0(r)$ is the site density function which describes the spatial arrangement of acceptors around the donor. For a dipole–dipole energy transfer, $W(r)$ may be defined as^{21–23}

$$W(r) = \frac{3}{2} \kappa^2 \frac{1}{\tau_0} \left(\frac{R_0}{r}\right)^6 \quad (3)$$

with τ_0 the lifetime of the isolated donor, κ the anisotropic factor

containing the angular dependence of the dipolar interaction, and R_0 the critical energy transfer radius. R_0 is defined as^{21–24}

$$R_0^6 = \frac{9000 \ln 10 \kappa^2 Q_D}{128 \pi^6 n^4 N_A} \int \frac{F_D(\nu) \epsilon_A(\nu)}{\nu^4} d\nu \quad (4)$$

where N_A is Avagadro's number, n is the refractive index of the embedding medium, $\epsilon_A(\nu)$ is a molar extinction coefficient of the acceptor, and $F_D(\nu)$ is the fluorescence intensity, and Q_D the fluorescence quantum yield of the donor. In the limit of an infinite system with random acceptor distribution, $\rho_0(r) = \rho_0$, and we can write the survival probability as^{21–23}

$$\Phi_D(t) = \exp\left[\frac{t}{\tau_0} - A_0 \Gamma\left(1 - \frac{d}{6}\right) \left(\frac{t}{\tau_0}\right)^{d/6}\right] \quad (5)$$

where d is the dimension of the embedding medium, Γ is the gamma function, and A_0 is the energy-transfer prefactor^{21–23}

$$A_0 = p \rho_0 C \pi R_0^d \quad (6)$$

A_0 defines the number of acceptors within a sphere of radius R_0 with C a constant that depends on d (e.g., for $d = 3$, $C = 4/3$ for a sphere and $C = 2/3$ for a hemisphere).

An alternative mechanism for energy transfer, the exchange interaction, has also been considered. In exchange interaction, $W(r)$ falls off exponentially with distance and the interaction is very short range. This leads to a markedly different behavior for $\Phi(t)$, which we have attempted to fit to our data.²⁰ The temporal dependence of the data is not, however, described by this model.

We show that a spectral overlap between the emission of naphthalene and 2-methoxynaphthalene and the optical absorption of silica defects exists. On the basis of the energy of the defect absorption, we suggest that the defects are peroxide radicals (Si–O–O*) and peroxide bridges (Si–O–O–Si) in the lattice.^{25,26} Other defect sites such as oxygen vacancies and dangling hydroxyl groups have absorption energies that do not overlap with the adsorbates' emission and probably do not interact with these molecules. The survival probability of the fluorescence of the adsorbed aromatics is also measured and fit to eq 5. From this, values for τ_0 and A_0 are determined. The value for R_0 may be calculated from the overlap if a reasonable value for the quantity $p \rho_0$ is assumed.

The presence of dipole–dipole energy-transfer interactions between the silica gel defects and excited aromatic probe molecules offers an appealing explanation for the nonexponential relaxation of the probe fluorescence. From the dipole–dipole model, we are able to define a single lifetime, τ_0 , for the adsorbate excited state which we find depends on the density of dangling hydroxyl groups on the surface. The nonexponential relaxation arises from en-

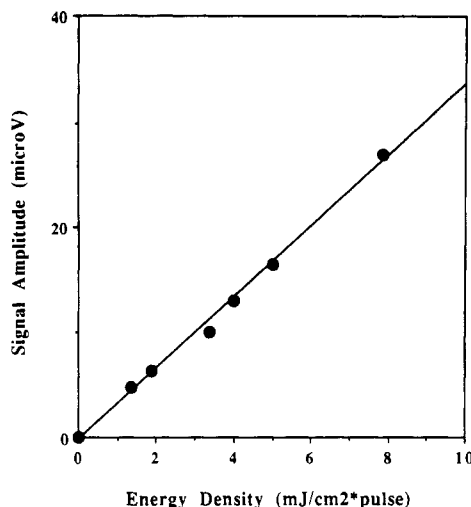


Figure 1. Linearity of the photothermal deflection signal as a function of the energy density of excitation.

ergy-transfer interactions with randomly distributed acceptor defect sites in silica gel.

Experimental Section

The silica gel used in these experiments was silica gel 60 obtained from E. Merck (Darmstadt, Germany). It has an average pore radius of 35 Å and a BET surface area of $390 \pm 10 \text{ m}^2/\text{g}$.^{4,27} Two sets of samples were heated in a tube furnace to either 165 or 600 °C. The samples heated to 165 °C (SG165) have 2.9 vicinal and 1.5 isolated surface hydroxyl groups per nm^2 while those heated to 600 °C (SG600) have 1.5 isolated groups per nm^2 . These values were determined by heating the silica gel to 800 °C to obtain the total surface hydroxyl concentration by thermogravimetric analysis (TGA). The water loss at 165 and 600 °C was further estimated using TGA. At 165 °C only those water molecules physisorbed to the surface are desorbed while at higher temperatures the removal of hydroxyl groups by geminate dehydrogenation occurs.^{4,27} After heat treatment, the solids were stored under nitrogen until used.

Naphthalene and 2-methoxynaphthalene were obtained from Aldrich and used without further treatment. These were adsorbed to the silica gel 60 from isooctane solutions. Adsorption was done in sealed air-tight vials where the samples were allowed to sit without agitation until equilibrium was reached (approximately 1 h). The supernatant was decanted from the samples and the wet powder was dried under vacuum at 50 °C for 30 min. The adsorption of the organic by the solids was calculated from the difference between the optical absorption of the starting solutions and that of the equilibrium supernatant. The samples used in these studies contained between 5 and 20 $\mu\text{M}/\text{g}$ silica gel which is a surface density of $(0.7\text{--}3.1) \times 10^{-2} \text{ nm}^{-2}$. Samples were stored in air-tight vials and 2-methoxynaphthalene samples were stored in the dark to avoid photodegradation. We found that samples could be stored for months without any change in their photo-physical behavior.

The absorption spectrum of silica gel defects from 278 to 337 nm (35970 to 29670 cm^{-1}) was measured using photothermal deflection spectroscopy as described previously.^{20,27,28} The silica gel samples were pressed into a $<500 \mu\text{m}$ thick disk and suspended in isooctane solution at room temperature. The 10-ns output of a 10-Hz Nd:YAG pumped dye laser was frequency doubled and used to excite the defects. The energy density used was approximately $7.5 \text{ mJ pulse}^{-1} \text{ cm}^{-2}$. The energy density was varied using neutral-density filters, and the deflection signal was shown to increase linearly with energy density for values under $10 \text{ mJ pulse}^{-1} \text{ cm}^{-2}$ (see Figure 1). High energy densities of UV light have been shown previously to produce defects in quartz through multiphoton processes.³⁰⁻³²

The decay of the sample luminescence was monitored using time-correlated single photon counting (TCSPC) instrumentation which has been described elsewhere.^{4,20,27} A Coherent mode-locked

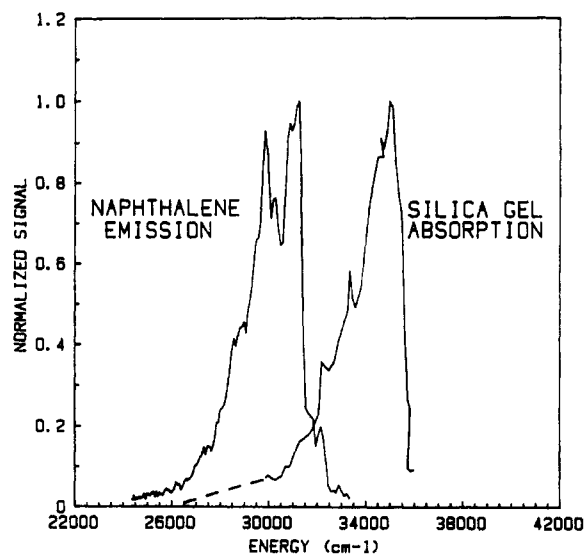


Figure 2. Spectral overlap between silica gel 60 absorption measured using photothermal deflection spectroscopy and naphthalene emission measured using the SLM-Aminco 4800S.

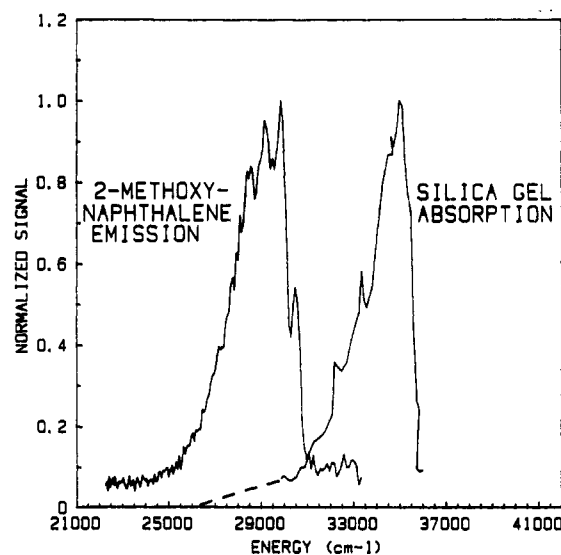


Figure 3. Spectral overlap between silica gel 60 absorption measured using photothermal deflection spectroscopy and 2-methoxynaphthalene emission measured using the SLM-Aminco 4800S.

argon ion laser synchronously pumping a cavity-dumped dye laser provided a 757-kHz train of 5-ps (fwhm) pulses at 575 nm which was frequency doubled to 287.5 nm (34783 cm^{-1}) and used to excite the sample. The energy density of light used for these experiments was $<1 \text{ nJ pulse}^{-1} \text{ cm}^{-2}$. The emission was collected and detected using standard TCSPC techniques. During the measurements, the samples were under vacuum ($<1 \text{ mTorr}$).

The temporal dependence of sample fluorescence decay was fit to model equations by a nonlinear least-squares optimization using a Marquadt-Levenberg algorithm. Minimization was done on the χ^2 function and the calculated values of the theoretical model were used as weighting factors. Different statistical functions including χ^2 ($=1, 1.5$), the Durbin-Watson factor ($DW = 2$), the skewness factor ($SKW = 0$), the kurtosis factor ($KUR = 3$), the weighted residual, and the autocorrelation of the weighted residual were calculated to determine the uniqueness of the fit to the model equations.

The steady-state emission spectra of the samples were taken using an SLM-Aminco 4800S emission spectrometer.

Results and Discussion

Figures 2 and 3 show the overlap between the peroxide defect absorption and the emission from naphthalene and 2-methoxynaphthalene. Since the shape of the absorption spectrum for both

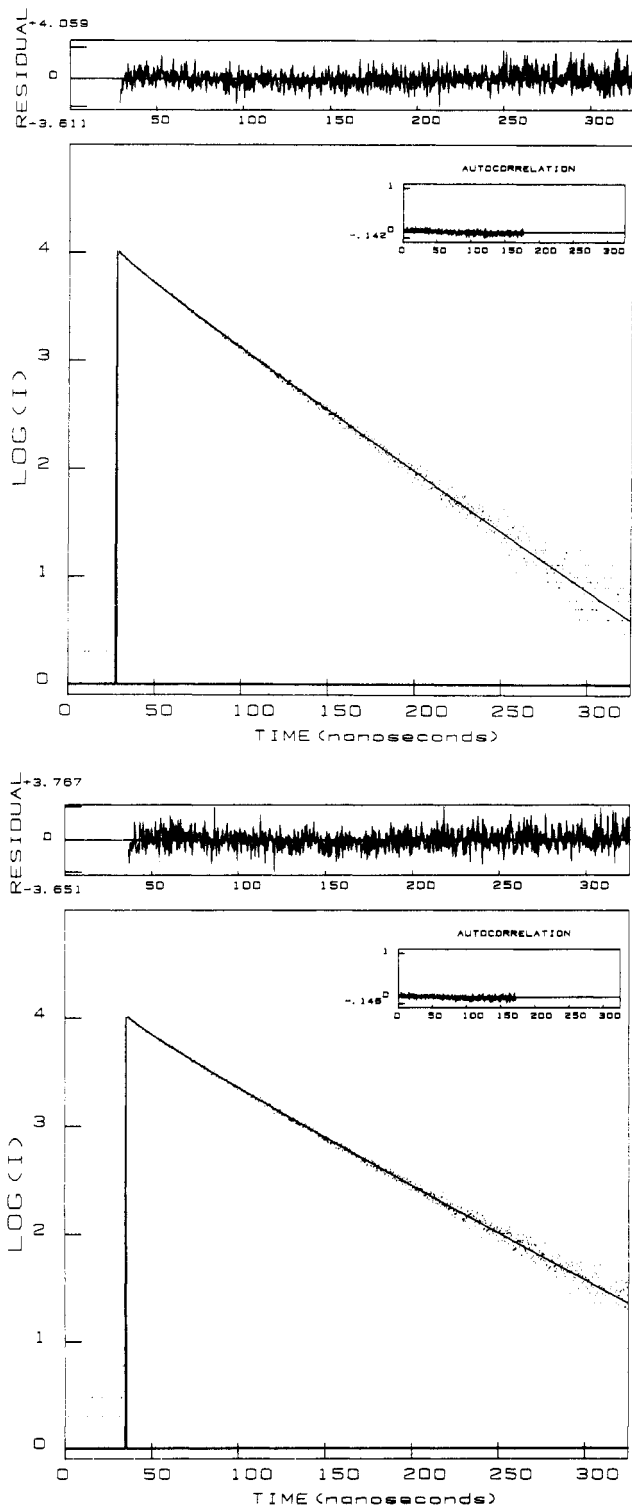


Figure 4. Survival probability of excited naphthalene adsorbed to silica gel 60 fit to the direct energy transfer model (eq 5): (a, top) heated to 165 °C with fitting statistics $\chi^2 = 1.30$, DW = 1.88, SKW = 0.31, KUR = 3.36, and (b, bottom) heated to 600 °C with fitting statistics $\chi^2 = 1.20$, DW = 1.94, SKW = 0.25, KUR = 3.27.

the SG165 and the SG600 are the same, only the SG165 is shown. The red edge of the absorption has been extrapolated as an exponential Urbach edge as discussed elsewhere.²⁶ On the basis of the energy of the adsorption, we may identify the defects interacting with the adsorbates as peroxide defects.

The survival probabilities of the excited probe molecules adsorbed to SG165 and SG600 are shown in Figures 4 and 5. The data have been fit to the dipole-dipole model (eq 5) where we have set $d = 3$. The values for τ_0 and A_0 determined by these fits are listed in Table I along with the lifetime measurements made for the probe molecules in solution. The fluorescence re-

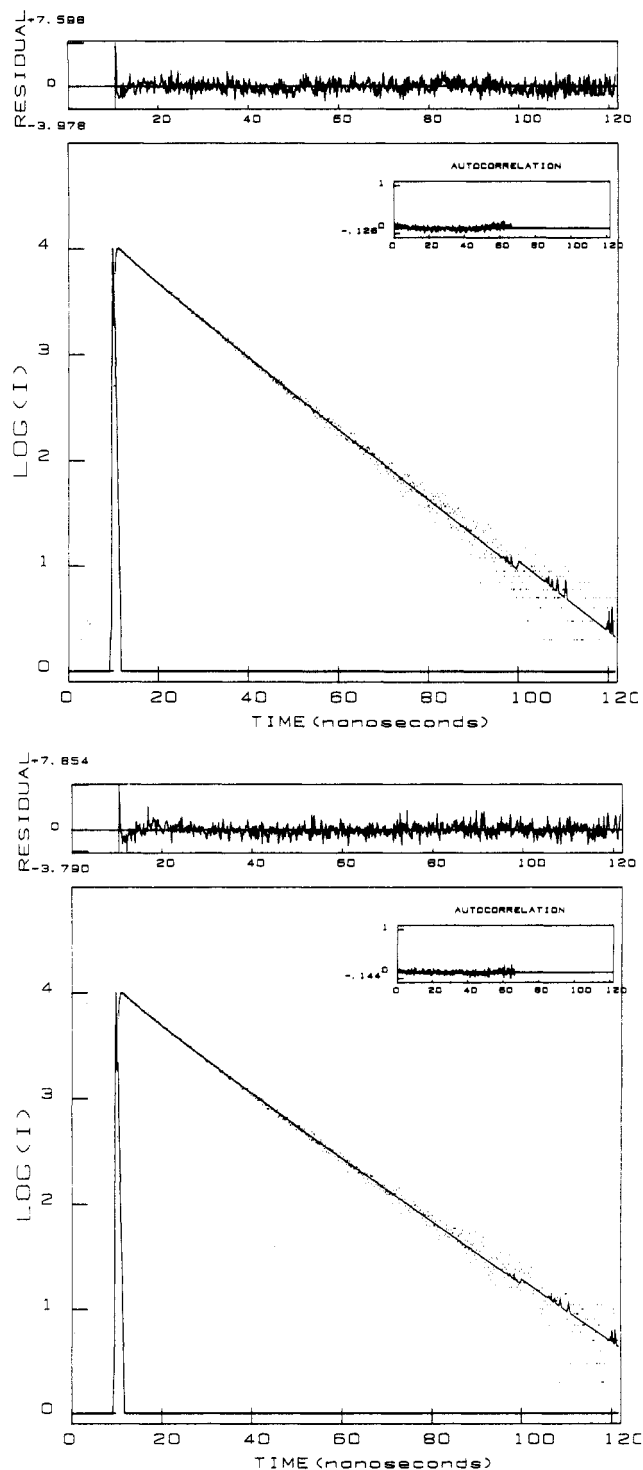


Figure 5. Survival probability of excited 2-methoxynaphthalene adsorbed to silica gel 60 fit to the direct energy transfer model (eq 5): (a, top) heated to 165 °C with fitting statistics $\chi^2 = 1.39$, DW = 1.92, SKW = 0.62, KUR = 5.72, and (b, bottom) heated to 600 °C with fitting statistics $\chi^2 = 1.37$, DW = 1.79, SKW = 0.61, KUR = 6.27.

laxation for all molecules observed in solution was found to be exponential. Fitting the relaxations of the adsorbed molecules to an exponential function gave very poor results.

For dipole-dipole energy transfer, we may calculate the maximum distance probed by the energy-transfer process, R_{\max} , which is determined by the radiative damping process, τ_0 . R_{\max} may be defined as $R_{\max} = (3/2)\kappa^2(1/\tau_0)R_0^6$,^{4,23} and we can show that $R_{\max} \sim 1.45R_0$. R_0 can be estimated to be 10 Å for naphthalene and 2-methoxynaphthalene, which is the same as found for the defect sites in silicalite. We calculate R_0 by evaluating the overlaps shown in Figures 2 and 3, assuming a maximum value for ϵ_A of $35 \text{ cm}^{-1} \text{ M}^{-1}$ which is consistent with our work with silicalite²⁰

TABLE I: Results of Fitting Survival Probabilities Measured to Eq 5 or an Exponential Function (Solution Samples)

probe molecule	system	lifetime, t_0 (ns)	prefactor, B
naphthalene	isooctane	104.0 ± 0.5	
	acetonitrile	93.4 ± 0.3	
	ethanol	93.9 ± 0.2	
	air-equilibrated ethanol	31.1 ± 1.0	
	SG600	53.9 ± 0.4	0.20 ± 0.01
2-methoxynaphthalene	SG165	41.9 ± 0.3	0.18 ± 0.01
	isooctane	14.3 ± 0.1	
	acetonitrile	13.1 ± 0.1	
	SG600	15.6 ± 0.2	0.17 ± 0.01
	SG165	13.7 ± 0.1	0.13 ± 0.01

and with recent results of Devine.³⁰ R_{\max} for these systems is therefore approximately 15 Å, suggesting that defects both on the silica particle surface and in the bulk should be probed. This supports setting $d = 3$ in eq 5, as R_{\max} is too small to allow interaction across the pore volume ($R_p = 35$ Å). The interactions probed are within a hemisphere centered at the donor position on the pore surface.

In porous media, direct energy transfer can demonstrate a crossover in effective geometry. The crossover is associated with a characteristic time, t_{cross} , which in this system is related to the time at which interactions across the pore volume become important.^{4,23} t_{cross} may be approximated by $(2R_p/R_0)^6\tau_0$. For silica gel 60, we calculate $t_{\text{cross}} > 1$ μs, which also confirms that the interaction across the pore volume are unimportant during the excited donor lifetimes ($\tau_0 < 100$ ns).

We can use eq 6 to calculate the number of defects in the silica gel system with the values of A_0 and R_0 determined. We find values for the defect density between 0.5×10^{20} and 2.0×10^{20} cm⁻³ depending on the system analyzed. This suggests that the error of the calculation is approximately a factor of 2, in contrast to the fits to the relaxation data (see Table I) which suggest a precision of a few percent. The range of values determined for the defect density in silica gel is on the same order of magnitude as that found in silicalite, 3×10^{20} cm⁻³.²⁰

The defect density determined for the silica gel 60 gives an average distance between defects, assuming a random distribution, of 17–27 Å. This density of defects is large, suggesting that either there are a large number of defects in the bulk of the silica particles or the adsorbates are positioned where there is a higher local concentration of defects. There is evidence that the defect concentration is higher at the surface and the silica defects observed behave as surface defects.²⁶ Because the adsorbates are located on the particle surface, we would expect that the density determined from the energy-transfer prefactor would reflect this higher local concentration.

The fluorescence lifetimes, τ_0 , measured for naphthalene adsorbed to silica gel are found to be shorter than that in solution (see Table I). This indicates that the adsorption of the molecules at an interface affects the fluorescence lifetime of the molecules. In addition, the lifetimes measured for both naphthalene and 2-methoxynaphthalene were shorter for the molecules adsorbed to SG165 than for those on SG600 indicating that the surface hydroxyl groups play a role in the binding. At very low surface coverage in the SG165, the adsorbates will bind preferentially to the vicinal sites where there are 2 hydroxyls per adsorbate. In the SG600, the binding sites have only 1 hydroxyl per adsorbate. The vicinal sites offer more extensive hydrogen binding which may be correlated to fluorescence quenching.

The relaxation dynamics of molecules embedded in solid supports have been observed by many investigators to behave differently than in homogeneous phases, and nonexponential relaxation behavior for aromatic adsorbates has been observed in a number of other studies.^{6–10} This behavior has been previously attributed to heterogeneities on silica gel surfaces; these heterogeneities are thought to provide a range of environments for the adsorbates. It has further been assumed that the excited adsorbate relaxation is sensitive to the polarity and the local

dielectric of the adsorption sites. In this picture, the excited molecules relax at different rates and the system is characterized not by a single lifetime but a distribution of lifetimes.^{14–17}

Some authors have fit their data assuming a form for a lifetime distribution and have determined a mean value for the relaxation time and a width of the lifetime distribution. For example, Krasnansky et al. have recently studied the fluorescence from pyrene and 9,10-diphenylanthracene adsorbed to Cabosil and have found the survival probability to be nonexponential.⁸ To describe their data, they have used the model developed by Albery et al.¹⁴ and Scott¹⁵ which assumes the molecules show a Gaussian distribution of lifetimes.

Previously, Bauer et al. have used a biexponential function to fit the fluorescence relaxation of naphthalene and pyrene adsorbed to silica gel.^{6,7,9} They note that there is no physical interpretation for the biexponential but use the model to determine a mean lifetime for the processes based on a weighted average of the two lifetimes obtained from the fit. For naphthalene, this value is 49.1 ns. These authors claim that the adsorbates are distributed in a range of environments due to interactions with randomly distributed surface hydroxyl groups. In their explanation, this causes nonexponential relaxation of the adsorbate which is approximated by a biexponential function.^{16,17}

In this study, we have suggested that there is direct energy transfer between excited adsorbates and intrinsic defects in silica substrates including silica gel 60. We have demonstrated that there is an overlap between the adsorbate emission and defect absorption for the probe molecules studied. The dipole–dipole coupling model gives excellent fits to the observed nonexponential survival probability. In contrast to models that suggest a distribution of lifetimes arising from site heterogeneities, the dipole–dipole coupling model predicts a nonexponential survival probability due to a distribution of adsorbate–defect distances that cause a hierarchy of relaxation times. We emphasize that this is a specific interaction that quenches the fluorescence and propose that the radiative process for all adsorbate molecules in the absence of defects is characterized by a single lifetime, τ_0 .

Finally, we note that not all excited molecules adsorbed to silicas undergo energy transfer with defects. This strictly occurs for molecules in which a spectral overlap may be demonstrated. For example, the relaxations of rhodamine 6G adsorbed to silica gel have been found to be perfectly exponential and to give the same lifetimes as are found in solution.⁴ The emission of this molecule is in the red ($\lambda_{\max} > 540$ nm) so that the silica gel peroxide defect absorption does not have a significant overlap with it as the absorption due to the fact that the Urbach edge falls off exponentially throughout this region.²⁶

Conclusion

The direct energy transfer between aromatic molecules adsorbed to silica gel 60 and peroxide defect sites in silica gel has been demonstrated. Spectral overlap between the defect absorption and adsorbate emission is measured and used to confirm the presence of energy transfer. The energy transfer is shown to be responsible for the observed nonexponential relaxation of the adsorbate fluorescence. This is a new interpretation for the nonexponential relaxation that has been previously explained by adsorption site heterogeneity. The fluorescence lifetimes of adsorbed molecules are found to be affected by the number of hydroxyl groups on the silica surface. Values for the critical radius of energy transfer, R_0 , are determined to be approximately 10 Å and the density of peroxide defects is calculated to be $(0.5–2.0) \times 10^{20}$ cm⁻³.

Acknowledgment. We thank Prof. J. Klafter and Dr. P. Levitz for many enlightening discussions. A.R.L. thanks the N.I.H. for an N.R.S.A. training fellowship and Exxon Research and Engineering for generous support of this work.

Registry No. Naphthalene, 91-20-3; 2-methoxynaphthalene, 93-04-9.

References and Notes

- (1) Turro, N. J.; Zimmt, M. B.; Gould, I. R. *J. Am. Chem. Soc.* **1985**, *107*, 5826–5827.

- (2) Turro, N. J.; Gould, I. R.; Zimmt, M. B.; Cheng, C. C. *Chem. Phys. Lett.* **1985**, *119*, 484-488.
- (3) Drake, J. M.; Levitz, P.; Turro, N. J.; Nitsche, K. S.; Cassidy, K. F. *J. Phys. Chem.* **1988**, *92*, 4680-4684.
- (4) Levitz, P.; Drake, J. M.; Klafter, J. *J. Chem. Phys.* **1988**, *89*, 5224-5236.
- (5) Even, U.; Rademann, K.; Jortner, J.; Manor, N.; Reisfeld, R. *Phys. Rev. Lett.* **1984**, *52*, 2164-2167.
- (6) Bauer, R. K.; Mayo, P. d.; Natarajan, L. V.; Ware, W. R. *Can. J. Chem.* **1984**, *62*, 1279-1286.
- (7) Bauer, R. K.; Mayo, P. d.; Okada, K.; Ware, W. R.; Wu, K. *J. Phys. Chem.* **1983**, *87*, 460-466.
- (8) Krasnansky, R.; Koike, K.; Thomas, J. K. *J. Phys. Chem.* **1990**, *94*, 4521-4528.
- (9) Bauer, R. K.; Mayo, P. d.; Ware, W. R.; Wu, K. C. *J. Phys. Chem.* **1982**, *86*, 3781-3789.
- (10) Francis, C.; Lin, J.; Singer, L. *Chem. Phys. Lett.* **1983**, *94*, 162-167.
- (11) Liu, X.; Iu, K.-K.; Thomas, J. K. *J. Phys. Chem.* **1989**, *93*, 4120-4128.
- (12) Beck, G.; Thomas, J. K. *Chem. Phys. Lett.* **1983**, *94*, 553-557.
- (13) Yang, C.; El-Sayed, M. A.; Suib, S. L. *J. Phys. Chem.* **1987**, *91*, 4440-4443.
- (14) Albery, W. J.; Bartlett, P. N.; Wilde, C. P.; Darwent, J. R. *J. Am. Chem. Soc.* **1985**, *107*, 1854-1858.
- (15) Scott, K. F. *J. Chem. Soc., Faraday Trans.* **1980**, *76*, 2065-2079.
- (16) James, D. R.; Liu, Y. S.; Mayo, P. d.; Ware, W. R. *Chem. Phys. Lett.* **1985**, *120*, 460-465.
- (17) James, D. R.; Ware, W. R. *Chem. Phys. Lett.* **1986**, *126*, 7-11.
- (18) Basche, Th.; Brauchle, C. *J. Phys. Chem.* **1988**, *92*, 5069-5072.
- (19) Basche, Th.; Sauter, B.; Brauchle, C. *Ber. Bunsenges. Phys. Chem.* **1989**, *93*, 1055-1058.
- (20) Leheny, A. R.; Turro, N. J.; Drake, J. M. *J. Chem. Phys.*, in press.
- (21) Klafter, J.; Blumen, A. *Chem. Phys. Lett.* **1985**, *119*, 377-382.
- (22) Klafter, J.; Blumen, A. *J. Lumin.* **1985**, *34*, 77-82.
- (23) Drake, J. M.; Klafter, J.; Levitz, P. *Science* **1991**, *251*, 1574-1579.
- (24) Forster, T. *Discuss. Faraday Soc.* **1959**, *27*, 7-17.
- (25) Tsai, T. E.; Griscom, D. L. *Phys. Rev. Lett.* **1991**, *67*, 2517.
- (26) Leheny, A. R.; Turro, N. J.; Drake, J. M. Manuscript in preparation.
- (27) Drake, J. M.; Levitz, P.; Klafter, J. *Isr. J. Chem.* **1991**, *31*, 135-146.
- (28) Jackson, W. B.; Amer, N. M.; Boccara, A. C.; Fournier, D. *Appl. Opt.* **1981**, *20*, 1333.
- (29) Tam, A. C. *Rev. Mod. Phys.* **1986**, *58*, 381.
- (30) Devine, R. A. B. *Phys. Rev. Lett.* **1989**, *62*, 340.
- (31) Tsai, T. E.; Griscom, D. L.; Friebele, E. J. *Phys. Rev. Lett.* **1988**, *61*, 444-446.
- (32) Stathis, J. H.; Kastner, M. A. *Phys. Rev. B* **1984**, *29*, 7079-7081.

Condensation and Evaporation of H₂O on Ice Surfaces

D. R. Haynes, N. J. Tro,[†] and S. M. George*

Department of Chemistry and Biochemistry, University of Colorado, Boulder, Colorado 80309-0215
(Received: March 31, 1992; In Final Form: June 24, 1992)

The condensation and evaporation coefficients for H₂O on ice surfaces were measured using optical interference techniques. The condensation coefficient, α , was determined at ice surface temperatures from 20 to 185 K. For H₂O vapor at 300 K, the condensation coefficient decreased as a function of surface temperature from $\alpha = 1.06 \pm 0.10$ at 20 K to $\alpha = 0.65 \pm 0.08$ at 185 K. The temperature dependence of the condensation coefficient could be fit by a precursor-mediated adsorption model. The evaporation coefficient, γ , was obtained at various surface temperatures using isothermal desorption measurements. The evaporation coefficient was observed to be constant at $\gamma = 0.63 \pm 0.15$ for ice surface temperatures from 173 to 205 K. Over the temperature range where the condensation and evaporation coefficients could both be measured, α and γ were equivalent within the experimental error limits. This equivalence indicates that evaporation or condensation rates are dictated only by temperature and pressure and can be treated individually during net condensation, net evaporation, or steady-state equilibrium. An Arrhenius analysis of the H₂O isothermal desorption rates from ice at different temperatures revealed zero-order desorption kinetics expected for multilayer desorption. The activation barrier for desorption was $E_d = 11.9 \pm 0.2$ kcal/mol with a preexponential of $\nu_0 = 2.8 \times 10^{30} \pm 1.0 \times 10^{30}$ molecules/(cm² s). Quasi-equilibrium experiments also determined an enthalpy of sublimation for H₂O from ice of $\Delta H_{\text{sub}} = 11.8 \pm 0.2$ kcal/mol and an entropy of sublimation of $\Delta S_{\text{sub}} = 31.0$ cal/(K mol). The equivalency of the kinetic desorption barrier and the quasi-equilibrium enthalpy of sublimation indicates that there is no barrier for H₂O adsorption on ice surfaces. The measured condensation and evaporation coefficients predict the presence of polar stratospheric clouds over the Antarctic pole at 10-20 km. These measurements also reveal that ice surfaces in the polar stratosphere are very dynamic with H₂O condensation and evaporation rates of 10-1000 ML/s (1 ML = 9.8×10^{14} molecules/cm²) for equilibrium conditions between 180 and 210 K.

I. Introduction

The condensation and evaporation of H₂O vapor on both liquid water and solid ice has been studied for many years.¹⁻⁹ Interest in this topic is motivated by its significance in understanding how processes such as cloud formation and growth occur in the atmosphere.^{7,9-14} A detailed knowledge of the condensation and evaporation coefficients for H₂O on ice has increased in importance since recent atmospheric studies have revealed the role of heterogeneous chemistry on ice particles.¹⁰ In particular, the ozone hole over Antarctica in the spring is intimately linked with the presence of ice particles known as polar stratospheric clouds.¹⁵⁻¹⁷

Modeling of heterogeneous chemistry in the stratosphere is dependent on accurate condensation and evaporation coefficients. Unfortunately, experimentally derived values of the condensation coefficient extend from approximately $\alpha = 0.01$ ^{7,14,18} to $\alpha =$

1.0 .^{3,19-22} This considerable range of values can be attributed to the numerous techniques, experimental parameters, and theoretical assumptions that have been employed by the various studies. The temperature of the H₂O vapor and surface may also be very important, although no studies have established the dependence of the condensation coefficient on these parameters.

The condensation coefficient, α , and the evaporation coefficient, γ , are defined as

$$\alpha = C_{\text{exp}}/C_{\text{max}} \quad (1)$$

$$\gamma = E_{\text{exp}}/E_{\text{max}} \quad (2)$$

In these expressions, C_{exp} and E_{exp} are the experimental rates of condensation and evaporation, respectively. Likewise, $C_{\text{max}} = P_v(2\pi mkT_v)^{-1/2}$ and $E_{\text{max}} = P_s(2\pi mkT_s)^{-1/2}$ are the maximum theoretical rates of condensation and evaporation. P_v is the vapor pressure at temperature T_v , P_s is the vapor pressure that would be present for a system at equilibrium at a surface temperature

[†] Present address: Department of Chemistry, Westmont College, Santa Barbara, CA.